

Unveiling the atomic and electronic structure of the VN/MgO interface

Zaoli Zhang,¹ B. Rashkova,¹ G. Dehm,^{1,2} P. Lazar,³ J. Redinger,³ and R. Podlucky⁴

¹*Erich Schmid Institute of Materials Science, Austrian Academy of Sciences, Leoben, Austria*

²*Department Materials Physics, University of Leoben, Leoben, Austria*

³*Institute of Applied Physics, Vienna University of Technology, Vienna, Austria*

⁴*Department of Physical Chemistry, Vienna University, Vienna, Austria*

(Received 6 July 2010; published 16 August 2010)

We report a quantitative comparison of the interface structure of VN/MgO(001) using *ab initio* density-functional theory (DFT), aberration-corrected high-resolution transmission electron microscopy (HRTEM), and electron energy-loss spectroscopy (EELS). By HRTEM, we show an atomic resolution structure of epitaxially grown VN film on MgO with a clearly resolved oxygen and nitrogen sublattice across the interface. As revealed by DFT, the (002) interplanar spacing oscillates in the first several VN layers across the interface. Interfacial chemistry determined by EELS analysis shows the preponderance of O and V atom at the interface, resulting in a small detectable core-level shift.

DOI: [10.1103/PhysRevB.82.060103](https://doi.org/10.1103/PhysRevB.82.060103)

PACS number(s): 61.05.-a, 06.30.Bp, 68.37.Og, 79.20.Uv

Experimental studies have shown that transition-metal nitrides are extremely hard materials.¹⁻⁴ When they are applied as multilayers, their hardness (more than 40 GPa) exceeds the hardness of the constituent monophase nitrides.³ Such nitride coatings are promising for a variety of practical applications where high hardness and wear resistances are needed, for example, as hard coatings to protect cutting tools or as diffusion barriers in microelectronic device.³ However, to understand the mechanism causing superhardness including the stable interface configurations of transition-metal nitride coatings on substrates calls for comprehensive experimental studies on the atomic and electronic structure combined with atomic-level calculation, and a comparison at the atomic scale.

Lazar *et al.*⁵ calculated the elastic and mechanical properties of VN/TiN multilayers by density-functional-theory (DFT) approach. Recently, by *ab initio* DFT Zhang *et al.*⁶ studied the stress-strain response and electronic structure change during the tensile and shear deformation of superhard nanocomposite TiN-SiN-TiN systems, revealing a weakening of the Ti-N interplanar bonds next to the interface. Theoretical calculation also uncovers that N point defects could influence the stability and induce the atomic-scale structural changes in transition-metal nitrides accordingly.⁷

So far, the theoretical studies have gained insights into the atomic interface structure between metal nitride films and substrates, and have partially addressed the mechanism causing a hardness enhancement.⁸ However, the link to experimental observation is scarce.⁴ A preliminary experimental observation on the interface structure of VN/MgO(111) was carried out.⁹ Recently, using HRTEM and DFT calculations, Hultman *et al.*¹⁰ have shown that the SiN_x layers epitaxially grown on a TiN surface give rise to a strong interfacial bonding. Extended atomic-scale resolution observations, especially utilizing advanced spherical aberration-corrected (C_s-corrected) HRTEM technique,¹¹ are clearly needed. Moreover, a determination of the interfacial electronic structure as revealed by electron energy-loss spectroscopy (EELS) is also required.¹² In this Rapid Communication, we report a detailed study of atomic and electronic structures of the VN/MgO interface as revealed by C_s-corrected HRTEM

and displacement measurement together with energy-loss near-edge structure (ELNES) to get a complete experimental picture about the interface structure, which is then compared to DFT calculations.

We grew the VN film on MgO(001) substrate by using an unbalanced direct current magnetron sputtering system.¹³ Transmission electron microscopy (TEM) specimen was prepared by wedge Tripod polishing. A 200 kV field-emission TEM/STEM JEOL 2100F equipped with an image-side C_s-corrector and with an energy filter (Tridiem) was used. The energy resolution in EELS was 1.0 eV at 200 kV. EELS spectra were recorded in STEM mode simultaneously with annular dark field (ADF) image, and then carefully processed. For the DFT calculations, the Vienna *ab initio* simulation package VASP (Ref. 14) was applied using the generalized-gradient approximation as parametrized by Ref. 15. The (100) interface was modeled by a repeated slab scheme with 15 layers of MgO and VN, respectively. Two types of supercells were constructed: either a three-dimensional superlattice (...VN/MgO/VN/MgO...) or with vacuum layers between the VN/MgO building blocks. As a result the geometrical and electronic interface properties turned out to be independent of the chosen model, confirming that the chosen number of layers was sufficient. Concerning the in-plane lattice of the perfect interface a 1 × 1 cell was chosen. For estimating the effects of diffusion (i.e., substitutional defects) calculations for a c2 × 2 cell were done as well. In all cases all atomic positions were fully relaxed for a 11 × 11 × 1 (1 × 1 cell) and a 8 × 8 × 1 (c2 × 2 cell) k-point mesh. The chosen lateral lattice constant was 4.21 Å.

An overview of the VN/MgO interface, a corresponding low-magnification ADF STEM image, is shown as an inset in Fig. 1(a). It indicates the distinct different contrast of the VN film and the MgO substrate. C_s-corrected HRTEM images of the VN/MgO interface were recorded with the electron-beam parallel to the [110] and [100] direction, respectively, using negative C_s imaging conditions.¹¹ In the structural image acquired along [110] direction (Fig. 1) the O and N atom columns can be discriminated from their faint contrast compared to bright Mg and V atomic columns, and the corresponding atomic models are superposed. The inter-

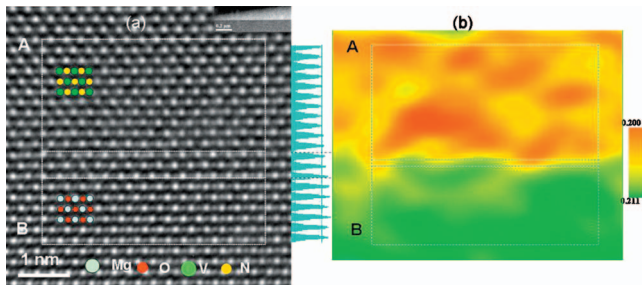


FIG. 1. (Color) (a) One HRTEM image of the VN/MgO interface with an epitaxial relationship, i.e., $\langle 100 \rangle$ (001) VN// $\langle 100 \rangle$ (001) MgO, recorded along $[110]$ direction using a negative C_S ($-3.0 \mu\text{m}$), in which the O and N atomic columns are clearly visible. The intensity profile (from A to B) obtained by integrating over a rectangular area reveals a jump in the intensity across the interface. (b) Color map of modulation of the 002 spatial frequency, showing the d_{002} spacing distribution across the interface. A low-magnification ADF STEM image is inserted in (a). The color code ranges from 0.200 to 0.211 nm.

face is atomically smooth and uniform across the entire specimen segment captured by TEM. The contrast difference between N and O atom is, however, too small to be distinguished from the phase contrast. By utilizing the profile analysis, the intensity variation across the interface is detectable [Fig. 1(a)], which changes within three atomic layers. However, using generalized geometrical phase analysis^{16,17} which can probe the tiny variation in lattice plane spacing

with unprecedented precision, the interface location can be unambiguously determined. Figure 1(b) is the map of modulation of the 002 spatial frequency, i.e., the (002) lattice plane spacing (d_{002}) distribution across the interface. A clear and abrupt change in the spacing is detected, which denotes the position of the interface.

The image along $[100]$ direction does not allow to discriminate the individual atom columns since they overlap. Figure 2(a) shows the corresponding HRTEM image. Under a certain experimental condition, however, a slight contrast variation across the interface due to the different atom potentials of VN and MgO can be identified, indicating the location of the interface. One part of the *ab initio* DFT calculated atomic model in $[100]$ projection is shown in Fig. 2(c). The $3.5 \times 3.5 \times 3.5 \text{ nm}^3$ large structure model covers $16d_{002}$ spacings in total and is used for further analysis. The corresponding HRTEM potential image of the interface is calculated [Fig. 2(b)] using the multislice image calculation, which faithfully represent the atomic structure of the interface. From the potential image, a sharp interface due to the potential difference is clearly visible. However, extensive HRTEM image calculations further show that the interface along $[100]$ can be well identified only when an appropriate specimen thickness and defocus are applied, which is in accordance with the experimental observation.

For quantitatively comparing the predicted with observed interface structure, geometrical phase analysis was performed on the experimental image [Fig. 2(a)] and calculated image [Fig. 2(b)] to map the atom displacement across the

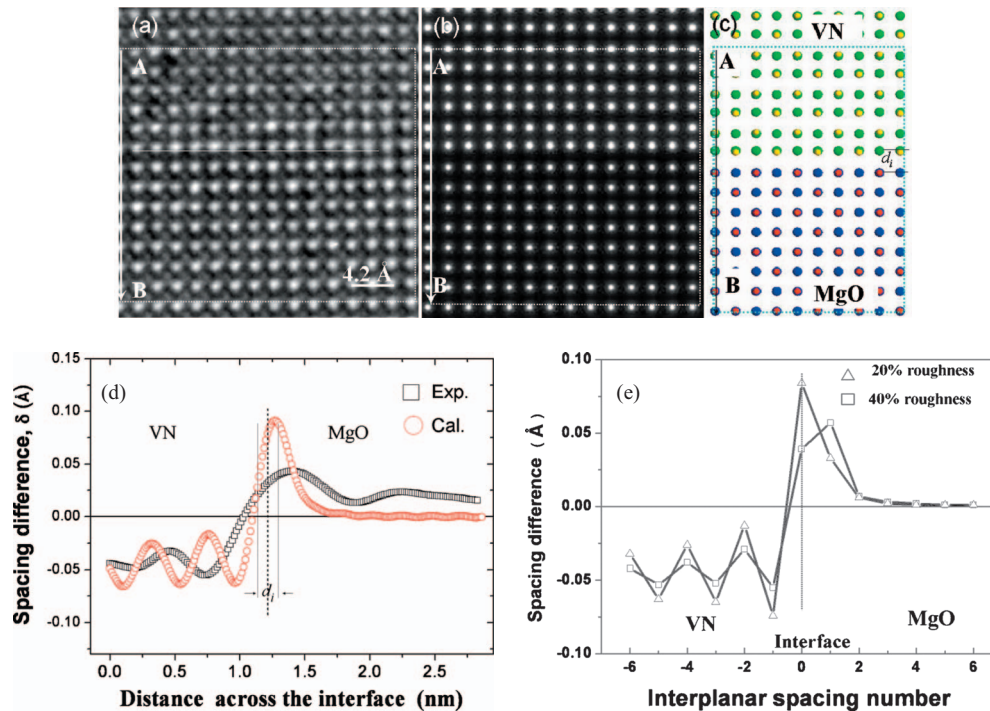


FIG. 2. (Color) (a) A segment of a HRTEM image of the VN/MgO interface recorded along $[100]$. In this projection, the V, N and Mg, O atom columns overlap and cannot be discriminated. The thickness is determined to be around 3.3 nm. A simulated potential image is shown in (b) based on an atomic model (c) obtained from *ab initio* calculation. The spacing difference (d) obtained by averaging over a rectangular area (as denoted by dotted lines) of around 3.0 nm from A to B in (a), (b), and (c) is plotted as a function of distance covering 13 spacing of d_{002} , where the red and black curves denote the calculated (no roughness) and experimental results, respectively. The interfacial spacing d_i is schematically labeled. Panel (e) shows the effects of an assumed mono atomic step roughness (20%, 40% roughness).

interface. The 002 reflection, corresponding to the planes parallel to the interface, was used for atomic displacement analysis. The atom displacement distribution (not shown) obtained from the experimental image reveals an abrupt change in the interlayer spacing at the interface: a maximum approached from the MgO side of the interface and a dramatic decrease is found on the VN side. Away from the interface, the displacement gradually decreases, eventually reaching a constant value. The same evaluation procedure applied to the calculated potential image, in contrast, shows that the atom displacement oscillates in the VN layers. Even though the interlayer spacings determined experimentally and theoretically do not fully follow the same variations, they exhibit a similar tendency. For quantitative comparison, an averaged spacing difference¹⁸ is plotted as a function of distance across the interface from VN to MgO [Fig. 2(d)]. Clearly, the layer displacement at the interface differs and the measured displacement oscillations in VN and the contraction in MgO are smaller than the values derived from the DFT model. The discrepancies can be beam-induced interfacial atom relaxation during the experiment and local composition deviations, which are not included in the DFT structure determination. A simulation of a wider interface by considering a 50% substitutional exchange of O and N or Mg and V at the interface leads to an improved agreement between experiment and theory. However, the DFT calculations show an increase in interface energy of roughly 1 eV per exchanged atom. Monoatomic steps (roughness) at the interface, as another possible reason for the discrepancies, can be taken into account by a simple model considering a rigid shift for parts of the interface for just one atomic step. Results for different degrees of model roughness are shown in Fig. 2(e). Due to the drastic change in the layer spacing across the interface, shifting portions of the interface has a rather large net effect in reducing the effective spacing at the interface.

EELS line scan using a probe step of 0.5 nm was performed. The integrated intensity from O *K*, Mg *K*, and N *K*, V *L*_{2,3} edges were converted to relative concentrations using pure bulk MgO and VN as standards. Figure 3 shows elemental relative composition profiles across the interface over a distance at about 20 nm as determined by EELS.¹⁹ The profile indicates that the interface is chemically not abrupt. Moreover, the oxygen concentration is slightly shifted to the VN side whereas vanadium is shifted to the MgO side at the interface. Both O and V concentration are higher than those of Mg and N at the interface region. This indicates an enrichment of in O and V atoms at the interface as compared to the stoichiometric MgO and VN. This most likely corresponds to highly occupied O- and V-terminated lattice planes from each side. In other words, the V-O bonds may be dominant at the VN/MgO interface.

Using a probe smaller than 2 Å, a step size of 0.35 nm and a dispersion of 0.1 eV/channel, the ELNES of the V *L*_{2,3} and O *K* edges was recorded at a distance of ~6.6 nm across the interface. The V *L*_{2,3} and O *K* ELNES obviously change as the probe position moves from the VN film to the MgO substrate (Fig. 4). In general, V, N, and O ELNES exhibit typical features as previously shown.^{20,21} However, closely examining the spectra further reveals that the V *L*_{2,3} core level is slightly shifted to a lower energy position by

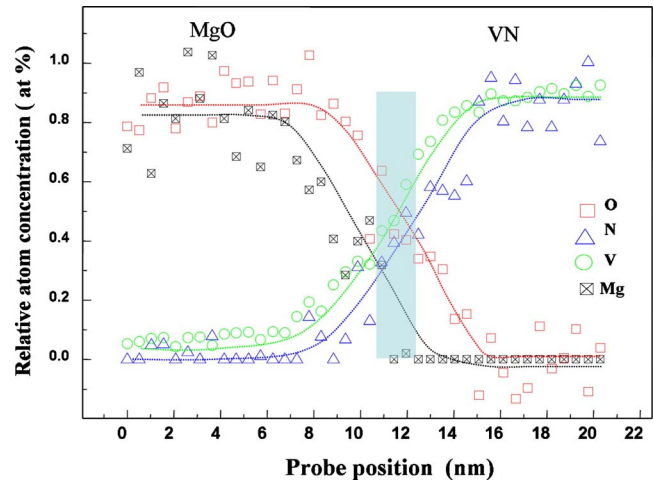


FIG. 3. (Color online) Elemental relative composition profiles across the interface obtained by EELS quantification show the integrated intensity for O *K*, N *K*, V *L*, and Mg *K* edges, normalized to bulk VN and MgO signals. The O, V intensity at the interface is higher than the Mg, N intensity, revealing a predominance of V and O. As the Mg *K* edge (1301 eV) was used for quantification, Mg data is more scattered. The fitting curves are denoted by the dotted lines. The shadow area roughly indicates the interface region.

~0.6 eV when approaching the interface region. This implies that the V valence state at the interface region is most likely slightly reduced as compared to those far away from the interface whereas for the O *K* peaks no noticeable energy

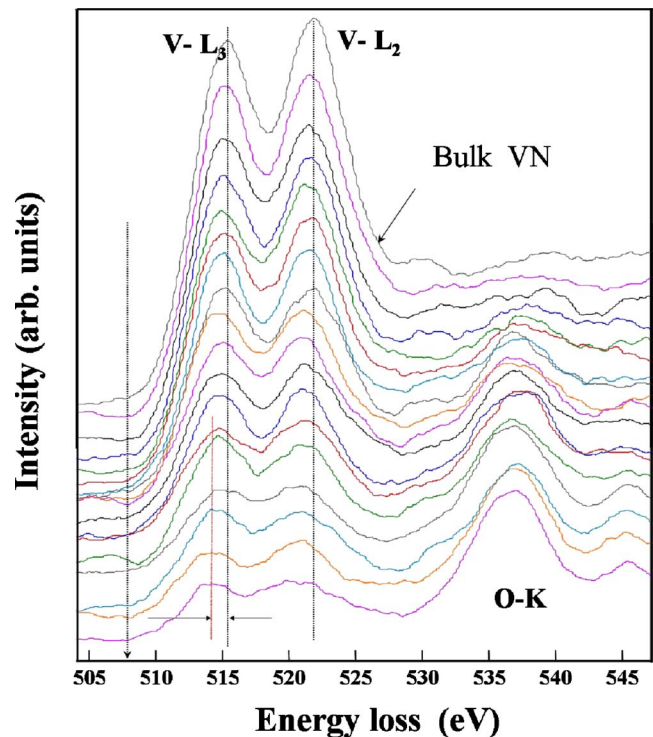


FIG. 4. (Color online) ELNES of V *L*_{2,3} and O *K* edges from the interface and next to the interface within several nanometers range. Note that the V *L*_{2,3} core-level shifts to lower energy by ~0.6 eV whereas the O *K* edge shows no significant change.

shift is found. The ratio of V L_3/L_2 also slightly varies from the VN film to the interface region. Using a step function to fit the V L_3 and L_2 edges, it is determined to be around (1.68 ± 0.04) in the bulk and (2.67 ± 0.33) at the interface region.¹⁹ The key features of the V $L_{2,3}$ ELNES resemble those of V oxide variants to a certain extent.²² This implies a dissimilar coordination of V at the interface as compared to the VN bulk.

According to EELS the predominant atomic species at the interface are V and O. This has been predicted by a DFT study of the VN/MgO(111) interface,⁹ which reveals that the V-O bond at the interface is by far the most stable configuration with the lowest interface adhesion energy. It demonstrates that V-O bonds at the interface are energetically most likely and preferable as compared with other interface terminations, which are in accordance with the elemental profiles and ELNES measurement.

Structural relaxation results in a local structural rearrangement at and near the interface. Such a local rearrangement can propagate into several lattice planes. This can be seen in the oscillations of interplanar distances, i.e., for the cube-on-cube VN/MgO in the (002) lattice planes in the DFT calculated interface structure. The experimental measurements reveal a similar phenomenon. It thus firmly corroborates that the interfacial structure within a few atomic layers slightly deviates from both bulk sides. Consequently, the corresponding electronic structures at and near the interface will be different compared to bulk. It can be speculated that these structure oscillations may be important for tuning the elastic properties of interface controlled materials such as multilayers. Moreover, it should be noted that the oscillations are

relatively small in the MgO substrate compared to VN. This may be a consequence of the high elastic constant of MgO and also indicate an instability against a tetragonal distortion in stoichiometric VN as a reaction to the epitaxial lattice mismatch strain.⁵

A recent theoretical study pointed out that due to valence charge-density oscillations the Ti-N interplanar bond length adjacent to the interface oscillates, which results in the variation in $d_{(111)}$, $d_{(110)}$, and $d_{(001)}$ lattice plane spacing.⁶ To a certain extent, there exists a similarity to the present study. However, to draw a clear conclusion that it originates from the identical mechanism needs further experimental and theoretical support.

In summary, we have shown the atomically resolved interfacial structure for an epitaxially grown VN film on MgO. In HRTEM images the interface appears atomically abrupt. The analysis of the atomic displacement reveals that the interplanar spacings oscillate adjacent to the interface in a similar way for both experimental measurements and DFT calculations. The interfacial chemistry derived from ELNES with subnanometer spatial resolution revealed a V- and O-enriched interface where V-O bonds are likely to be formed at the interface, resulting in a slightly reduced V valence state.

The authors thank Christian Mitterer and Kerstin Kutschej for providing the materials. Part of this study was financed by the Austrian Nanoinitiative (NanoInterface). Thanks are also given to Gabriele Moser and Herwig Felber for preparing TEM specimens, and Herbert Weinhandl for his help during the image simulation.

¹M. Shinn, L. Hultman, and S. A. Barnett, *J. Mater. Res.* **7**, 901 (1992).

²P. H. Mayrhofer, C. Mitterer, L. Hultman, and H. Clemens, *Prog. Mater. Sci.* **51**, 1032 (2006).

³S. Veprek and M. J. G. Veprek-Heijman, *Surf. Coat. Technol.* **202**, 5063 (2008).

⁴L. Hultman, *Vacuum* **57**, 1 (2000).

⁵P. Lazar, J. Redinger, and R. Podloucky, *Phys. Rev. B* **76**, 174112 (2007).

⁶R. F. Zhang, A. S. Argon, and S. Veprek, *Phys. Rev. Lett.* **102**, 015503 (2009); *Phys. Rev. B* **79**, 245426 (2009).

⁷L. Tsetseris, N. Kalfagiannis, S. Logothetidis, and S. T. Pantelides, *Phys. Rev. Lett.* **99**, 125503 (2007).

⁸S. Veprek, A. S. Argon, and R. F. Zhang, *Philos. Mag. Lett.* **87**, 955 (2007).

⁹P. Lazar, B. Rashkova, J. Redinger, R. Podloucky, C. Mitterer, C. Scheu, and G. Dehm, *Thin Solid Films* **517**, 1177 (2008).

¹⁰L. Hultman, J. Bareño, A. Flink, H. Söderberg, K. Larsson, V. Petrova, M. Odén, J. E. Greene, and I. Petrov, *Phys. Rev. B* **75**, 155437 (2007).

¹¹C. L. Jia and K. Urban, *Science* **303**, 2001 (2004).

¹²D. Muller, *Nature Mater.* **8**, 263 (2009).

¹³K. Kutschej, B. Rashkova, J. Shen, D. Edwards, C. Mitterer, and G. Dehm, *Thin Solid Films* **516**, 369 (2007).

¹⁴G. Kresse and J. Furthmüller, *Phys. Rev. B* **54**, 11169 (1996); G. Kresse and D. Joubert, *ibid.* **59**, 1758 (1999).

¹⁵J. P. Perdew, J. A. Chevary, S. H. Vosko, K. A. Jackson, M. R.

Pederson, D. J. Singh, and C. Fiolhais, *Phys. Rev. B* **46**, 6671 (1992).

¹⁶A. K. Gutakovskii, A. L. Chuvilin, and S. A. Song, *Bull. Russ. Acad. Sci. Phys.* **71**, 1426 (2007).

¹⁷M. J. Hytch, E. Snoeck, and R. Kilaas, *Ultramicroscopy* **74**, 131 (1998).

¹⁸The mean value obtained by averaging over the whole image area is used as a reference. The corresponding spacing difference (δ_i) for each interplanar spacing (d_i) is then obtained by subtracting the mean value (d_{mean}), i.e., $\delta_i = d_i - d_{mean}$.

¹⁹As V $L_{2,3}$ (509 eV) and O K (532 eV) edges are very close, the quantification for V and N was carried out by using the bulk VN and MgO as standards, and a special procedure was used to calculate the net O integrated intensity. The determination of the L_3/L_2 ratio is as follows: (i) firstly, the background is removed and (ii) secondly, the V L edges are fit with a double step continuum model. Finally, after the continuum subtraction, the WL intensities $I(L_3)$ and $I(L_2)$ are obtained by integration of the peaks under certain energy windows.

²⁰B. Rashkova, P. Lazar, J. Redinger, R. Podloucky, G. Kothleitner, S. Sturm, K. Kutschej, C. Mitterer, C. Scheu, and G. Dehm, *Int. J. Mater. Res.* **98**, 11 (2007).

²¹F. Hofer, P. Warbichler, A. Scott, R. Brydson, I. Galesi, and B. Kolbesen, *J. Microsc.* **204**, 166 (2001).

²²M. Wieske, D. S. Su, F. Beckmann, and R. Schlögl, *Catal. Lett.* **81**, 43 (2002).